
Wukong: A 100 Million Large-scale Chinese Cross-modal Pre-training Benchmark

Jiayi Gu^{1*}, Xiaojun Meng^{1*}, Guansong Lu¹, Lu Hou¹, Minzhe Niu¹, Xiaodan Liang^{2†},
Lewei Yao¹, Runhui Huang², Wei Zhang¹, Xin Jiang¹, Chunjing Xu¹, Hang Xu^{1†}

Abstract

Vision-Language Pre-training (VLP) models have shown remarkable performance on various downstream tasks. Their success heavily relies on the scale of pre-trained cross-modal datasets. However, the lack of large-scale datasets and benchmarks in Chinese hinders the development of Chinese VLP models and broader multilingual applications. In this work, we release a large-scale Chinese cross-modal dataset named Wukong, which contains 100 million Chinese image-text pairs collected from the web. Wukong aims to benchmark different multi-modal pre-training methods to facilitate the VLP research and community development. Furthermore, we release a group of models pre-trained with various image encoders (ViT-B/ViT-L/SwinT) and also apply advanced pre-training techniques into VLP such as locked-image text tuning, token-wise similarity in contrastive learning, and reduced-token interaction. Extensive experiments and a benchmarking of different downstream tasks including a new largest human-verified image-text test dataset are also provided. Experiments show that Wukong can serve as a promising Chinese pre-training dataset and benchmark for different cross-modal learning methods. For the zero-shot image classification task on 10 datasets, Wukong_{ViT-L} achieves an average accuracy of 73.03%. For the image-text retrieval task, it achieves a mean recall of 71.6% on AIC-ICC which is 12.9% higher than WenLan 2.0. Also, our Wukong models are benchmarked on downstream tasks with other variants on multiple datasets, e.g., Flickr8K-CN, Flickr-30K-CN, COCO-CN, et al. More information can be referred to <https://wukong-dataset.github.io/wukong-dataset/>.

1 Introduction

Pre-training large-scale models on big data, and fine-tuning them on downstream tasks, has become an emerging paradigm of artificial intelligence systems. Models such as BERT [7] and GPT [1] grow in popularity in the natural language processing community as they possess high transferability to a wide range of downstream tasks, yielding state-of-the-art performance. Recent works such as CLIP [35], ALIGN [14], and FILIP [53] further extend this paradigm to the joint Vision Language Pre-training (VLP) domain and show superior results over state-of-the-art methods on various downstream tasks. Meanwhile, VLP models can be easily adapted to multiple practical applications such as image search engines, multi-choice visual answering and image labelling. In general, this promising direction draws significant attention from both industry and academia to consider it as the path to the next-generation AI models.

Two reasons lead to the success of VLP models. On the one hand, more advanced model architectures such as ViT [8]/BERT [7] and training objectives like contrastive learning [12], are usually able

¹ Huawei Noah's Ark Lab * These two authors contribute equally.

² Sun Yat-sen University † Corresponding authors: xu.hang@huawei.com & xdliang328@gmail.com

to lift the powerful generalization and robustness capabilities of learned representations. On the other hand, thanks to the concurrent advancement in hardware [45, 16] and distributed training frameworks [28, 37, 38], more and more data can be fed into a large-scale model to improve the generalization, transferability and zero-shot capability. In either vision or language tasks, pre-training on larger-scale data such as JFT-300M [46] in image classification [39], C4 dataset in T5 [36], has been proven useful and critical for improving downstream task performance via transfer or prompt learning. In addition, recent work [14] has already shown the potential of scaling up the VLP model by more than 100 million noisy image-text pairs from the web.

Table 1: An overview of VLP datasets.

| Dataset | Language | Avail-ability | Image-text pairs |
|-------------------|----------------|---------------|--------------------|
| Flickr30k [55] | English | ✓ | 31,783 |
| CxC [32] | English | ✓ | 247,315 |
| SBU Captions [30] | English | ✓ | 1,000,000 |
| Product1M [58] | Chinese | ✓ | 1,000,000 |
| CC12M [2] | English | ✓ | 12,000,000 |
| RedCaps [6] | English | ✓ | 12,011,111 |
| YFCC100M [48] | English | ✓ | 99,200,000 |
| WIT [44] | multilingual | ✓ | 11,500,000 |
| LAION-400M [41] | English | ✓ | 400,000,000 |
| JFT-300M [46] | English | ✗ | 300,000,000 |
| JFT-3B [56] | English | ✗ | 3,000,000,000 |
| IG-3.5B-17k [27] | English | ✗ | 3,500,000,000 |
| M6-Corpus [22] | Chinese | ✗ | 60,500,000 |
| Wukong | Chinese | ✓ | 101,483,885 |

Therefore, the success of VLP models pre-trained on large-scale data urges people to continuously crawl and collect larger image-text datasets. Table 1 shows an overview of many popular datasets in the VLP domain. For English datasets, the publicly available Flickr30k [34], SBU Captions [31], and CC12M [42] are relatively small, while LAION-400M [41] is several magnitudes larger. Despite the availability of large-scale English datasets, directly translating them into Chinese and then training a Chinese VLP model can lead to a severe performance drop. We speculate this is due to the existence of many Chinese idioms and slang that simple translation cannot cover but brings errors that harm the performance. The current community lacks a large-scale publicly available dataset in Chinese, resulting in (a) the devel-

opment of the community being stunted; (b) secret large datasets used to achieve surprisingly good performance that other works cannot fairly compare with.

To bridge this gap, we release a large-scale Chinese cross-modal dataset named Wukong, which contains 100 million image-text pairs collected from the web. To guarantee the diversity and generalization, our Wukong dataset is collected according to a high-frequency Chinese word list with 200K queries. We also adopt image-based and text-based filtering strategies for further refinement. The resulting dataset is currently the largest Chinese vision-language dataset. We perform an analysis of this dataset and show that it covers a wide range of visual and textual concepts. Besides, we also build a test set called *Wukong-Test*, the quality of which has been verified by human experts. From the feedback, the image-text consistency is guaranteed in general even if all the data are collected on the web and only some simple filtering strategies are applied. Specifically, there are only about 2% image-text pairs are marked as weakly corresponding. Table 2 shows the comparison of available Chinese image-text testing datasets.

Table 2: Comparison of multimodal Chinese retrieval benchmarks.

| Dataset | #Images | #Texts |
|------------------------------|---------------|---------------|
| Flickr8K-CN _{Test} | 1,000 | 5,000 |
| Flickr30K-CN _{Test} | 1,000 | 5,000 |
| COCO-CN _{Test} | 1,000 | 1,053 |
| AIC-ICC _{Test-1} | 30,000 | 150,000 |
| AIC-ICC _{Test-2} | 30,000 | 150,000 |
| MUGE _{Test} | 30,399 | 5,004 |
| Wukong-Test | 33,365 | 33,365 |

Training a large-scale VLP model is quite expensive. For example, the largest CLIP [35] model takes 18 days to train on 592 NVIDIA-V100 GPUs and M6-10T [22] is trained on 512 NVIDIA-V100 GPUs for around 10 days. Thus it is almost impossible for everyone to pre-train a large-scale model due to substantial financial costs and hardware requirements. It is in great demand for researchers to download and reuse various kinds of pre-trained large-scale Chinese VLP models. However, the choices of publicly available large VLP models are also very limited, which hinders the improvement of performance on downstream tasks of large-scale models.

To contribute to the community, we release a group of dual-stream VLP models pre-trained using different image encoders (ViT [8] and SwinT [24]) and different pretraining techniques (CLIP [35], FILIP [53], and LiT [57]). We further provide an extensive Chinese benchmarking on various downstream tasks and datasets with hand-crafted Chinese labels, such as zero-shot image classification and image-text retrieval. Interestingly, though the frozen image encoders are trained on English image-text pairs, directly aligning them with a trainable Chinese text encoder still achieves remarkable

performance on downstream tasks. This also indicates the strong cross-lingual generalization of these pre-trained image encoders. Besides, we also find that using the cross-modal token-wise similarity from FILIP maintains the fine-grained word-patch alignment for various image encoders, even when they are frozen during the contrastive learning. Moreover, compared with the Chinese word-grained tokenization, we find that using character-grained tokenization in our models achieves better performance. More findings can be found in Section 5.

Experiments show that Wukong can serve as a promising Chinese pre-training dataset for different cross-modal learning methods. The pre-trained models show prominent performance on various downstream tasks such as zero-shot image classification and image-text retrieval. Specifically, our model Wukong_{VIT-L}, pre-trained using Wukong dataset, achieves up to 73.03% average top-1 accuracy on 10 datasets for zero-shot image classification. It also achieves 71.6% mean recall on AIC-ICC for image-text retrieval. This result is higher than that of WenLan 2.0, which is a Chinese image-text multimodal model pre-trained on its own large-scale dataset, by 12.9%.

In summary, our main contributions are:

- We release a large-scale Chinese VLP dataset with 100 million image-text pairs, covering a wide range of concepts. We also provide various benchmarking datasets with human-verified image-text pairs and Chinese labels for benchmarking the performance.
- We release a group of large-scale VLP models pre-trained with various popular architectures and methods. An extensive study and benchmarking are also provided.
- Our pre-trained model shows state-of-the-art performance on Chinese benchmarks such as zero-shot image classification and image-text retrieval tasks.

2 Related Work

Vision-Language Pre-training (VLP) Models. There are two typical architectures of VLP models according to the modality interaction methods, i.e., single-stream and dual-stream. Single-stream models [15, 19] directly concatenate the visual and textual embeddings together and feed them to a single transformer-based model. This kind of model can be easily fit into text/image generation tasks to perform image captioning or text-to-image generation, which are usually hard to evaluate and benchmark. Dual-stream models such as ViLBERT [26], CLIP [35], and ALIGN [14] have separate models for each modality. This paradigm is more flexible and efficient when modeling each modality, e.g., CNN for images and Transformers for texts. Moreover, dual-stream models have the merit of efficient inference for downstream tasks such as image-text retrieval, since the two encoders can be decoupled and the image/text features can be pre-computed offline. In CLIP [35], the authors also evaluate the image encoder as a self-supervised pre-trained model and show promising results. This paper mainly follows and benchmarks the dual-stream approaches.

Vision-Language Datasets. The current success of VLP models greatly lies in the scale of pre-trained datasets. The publicly available pre-training datasets used by recent VLP models are mainly image caption data or image-text pair data. Many small-sized datasets (e.g., a few hundred thousand) such as COCO-Captions [23], Flickr30k [34], Visual Genome [17], and VQA2 [11] are hand-annotated data that have very limited domain and diversity. On the other hand, pre-training models on online collected data (such as alt-texts from the HTML pages) have shown promising results. CC3M [42], CC12M [2] and YFCC100M [48] have millions of image-text pairs in English generated by an online data collection pipeline including image and text filters, as well as text transformations. VLP models on these datasets have shown to be effective in multiple downstream tasks. Moreover, larger-scale datasets with more than 100M samples (e.g., CLIP [35]: 400M and ALIGN [14]: 1.8B) have even armed the recent VLP models with surprisingly good zero-shot recognition ability, but they are not publicly available. In terms of vision-language datasets specifically for Chinese, as shown in Table 1, the dataset is either small-scale (Product1M [58]) or private (M6-Corpus [22]). Thus, the current community lacks a large-scale Vision-Language dataset in Chinese. We aim to contribute a Chinese dataset to benchmark various VLP methods.

3 Construction of Wukong Dataset

In this paper, we construct a dataset called Wukong containing 100 million image-text pairs collected from the web. To cover as diverse concepts as possible, a series of keywords are taken as the starting point. The original keyword list is taken from [43] and only the first 200,000 most frequently seen keywords are used. These keywords are then used to search for images and their corresponding

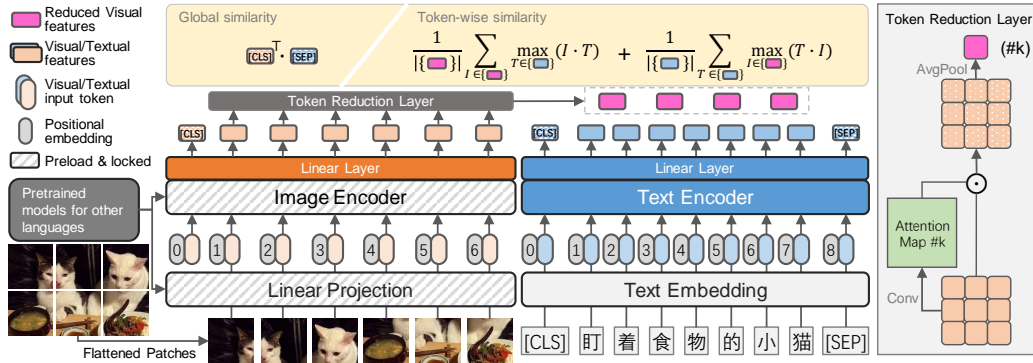


Figure 1: Overviews of our released models. Our Chinese pre-trained models consist of an image encoder and a text encoder with visual tokens and textual tokens as inputs. We have three variations of pretrained models: global similarity (CLIP-style); token-wise similarity (FILIP-style) and token-wise similarity with token reduction layer (Wukong-style).

captions in Baidu, a commonly used search engine for Chinese. For data balance, at most 1000 image-text pairs are kept for each keyword. In this way, we collect a total of 166 million raw (image, text) pairs. Then, following common practices [42, 2, 14], we apply a series of filtering strategies described in the sections below to finalize Wukong dataset. Some examples in our dataset can be found in the appendix. We also provide various benchmarking datasets with human-verified image-text pairs and Chinese labels for model benchmarks. Wukong-Test dataset contains 33k human-verified image-text pairs, which is currently the largest multimodal Chinese retrieval benchmark.

Image-based Filtering. We first filter the data according to the size and aspect ratio of the image. Only images with both dimensions greater than 200 pixels, and the ratio of large-to-small dimension of at most 3 are kept. In this way, we filter out images that are too small, too tall or too wide. This kind of image is of poor quality, especially after data augmentation processes such as upsampling or square cropping.

Text-based Filtering. Secondly, to select samples with high-quality Chinese descriptions of the corresponding image, we filter the data according to language, text length, and the frequency of text accompanying an image. Specifically, we first check the language and text length. We keep sentences that contain at least one but fewer than 32 Chinese characters. We also discard meaningless image descriptions like “000.jpg” from the text. Texts paired with too many images are usually irrelevant to the content of the images, like “查看源网页” (*View source page*), “展开全文” (*Expand text*), “摄影部落” (*Photography community*). In practice, we set this threshold as 10, i.e., we discard the image-text pairs whose text appears more than 10 times in the whole corpus collected. To protect the privacy of the individuals appearing in the text, we substitute person names with a special token “(人名)” (*Person name*). Besides, we also construct a list of Chinese sensitive words, and image-text pairs containing sensitive words are also discarded.

After applying the above filtering strategies, we finally get a dataset called Wukong for pre-training and a dataset called Wukong-Test for model testing. Table 3 shows the statistics of them.

Table 3: Statistics of datasets.

| | Image-text Pairs | Unique Tokens | Tokens per Caption | | |
|-------------|------------------|---------------|--------------------|-----|--------|
| | | | mean | std | median |
| Wukong | 101,483,885 | 20,442 | 22 | 7 | 24 |
| Wukong-Test | 33,365 | 5,155 | 22 | 7 | 24 |

4 Methodology

4.1 Text-Image Joint Alignment

Following the recent widely adopted contrastive pre-training architectures [35, 53], we use a dual-stream model with Transformer-based text and image encoders as shown in Figure 1. These two encoders convert textual and visual input tokens to embeddings of the same dimension. In this learned joint embedding space, we use a contrastive loss to encourage the paired image and text to have similar embeddings, while non-paired ones to have distinct embeddings.

4.2 Model Architectures

Visual Encoder. Two types of visual encoders, *i.e.*, Vision Transformer [8] (ViT) and Swin Transformer [24] (SwinT), are used as backbones for training different model variants. For ViT, the input image is first rescaled into a standard size and then split into fixed-size patches. Each patch is linearly embedded via a trainable linear projection. The resulting sequence of patch vectors is fed to a standard transformer encoder. Different from ViT, SwinT uses a hierarchical transformer that computes representation with shifted windows, which accelerates the original self-attention computation to non-overlapping local windows while also allowing for cross-window connection.

Textual Encoder. The textual encoder is a standard decoder-only transformer as in [35]. We use WordPiece [52] with a vocabulary size of 21,128 for Chinese text tokenization. Similar to [33], we add spaces around Chinese characters before applying WordPiece so that Chinese is effectively character-tokenized. We add two special tokens (*i.e.*, [CLS] and [SEP]) at the beginning and ending of each text sequence. The text encoder has 12 layers, each of which has 8 attention heads and a hidden state dimension of 512.

Linear Projection of the Encoders. On the top of the visual and textual encoders, the global representations of visual token sequence (e.g., [CLS] token for ViT; average pooled representation of all patch tokens for Swin Transformer) and textual token sequence (e.g., textual [SEP] token) are linearly projected to the common multi-modal space, followed by L2-normalization separately.

Token Reduction Layer. Instead of only computing the cross-modal similarity between global representations of sequences, we experiment with a late interaction method as introduced in FILIP [53]. We aim to take into account the fine-grained token-wise interaction between image patches and text tokens. It could potentially mine more detailed semantic word-patch alignment between two modalities. Meanwhile, as a large amount of computation is introduced by this token-wise interaction, we propose a token reduction layer inspired by [40]. It aims to learn a small set of tokens (e.g., 12 or 24) from the whole output tokens of the visual encoder (e.g., 16×16 in ViT-L/14), and use them for the reduced-token interaction. This token reduction layer is used in all the Wukong-style models.

4.3 Pre-training Objectives

Cross-modal contrastive learning, typically represented by CLIP [35], is one effective approach for training models using paired image-text data. It can learn representations of two modalities simultaneously by distinguishing the paired and unpaired samples. Given an image sample $\mathbf{x}^I \in \mathcal{I}$ and a text sample $\mathbf{x}^T \in \mathcal{T}$, the training objective is to make the learned image and text representations in the joint multi-modal space close if they are paired and far otherwise. For a training batch consisting of b image-text pairs $\{\mathbf{x}_k^I, \mathbf{x}_k^T\}_{k=1}^b$, \mathbf{x}_k^T (resp. \mathbf{x}_k^I) is positive to \mathbf{x}_k^I (resp. \mathbf{x}_k^T) while negative to all other texts (resp. images) in the same batch. Therefore, the image-to-text and text-to-image contrastive losses for $(\mathbf{x}_k^I, \mathbf{x}_k^T)$ can be formulated as $\mathcal{L}_k^I(\mathbf{x}_k^I, \{\mathbf{x}_j^T\}_{j=1}^b) = -\frac{1}{b} \log \frac{\exp(s_{k,k}^I)}{\sum_{j=1}^b \exp(s_{k,j}^I)}$ and $\mathcal{L}_k^T(\mathbf{x}_k^T, \{\mathbf{x}_j^I\}_{j=1}^b) = -\frac{1}{b} \log \frac{\exp(s_{k,k}^T)}{\sum_{j=1}^b \exp(s_{k,j}^T)}$ where $s_{k,j}^I$ denotes the similarity of the k -th image to the j -th text, while $s_{k,j}^T$ denotes the similarity between the k -th text to the j -th image. The total loss \mathcal{L} is then computed as $\mathcal{L} = \frac{1}{2} \sum_{k=1}^b (\mathcal{L}_k^I + \mathcal{L}_k^T)$. In this work, we explore two typical ways of measuring the similarity between an image and a text. The learned representations of the image and text are denoted as $\mathbf{z}^I \in \mathbb{R}^{n_1 \times d}$ and $\mathbf{z}^T \in \mathbb{R}^{n_2 \times d}$, respectively. Here n_1 and n_2 are the numbers of (non-padded) tokens in each image and text.

Global Similarity. In CLIP [35] and ALIGN [14], the similarity is computed via dot product of the global features of the entire image and text sequence. Specifically, the global similarity between the image and text is computed as $s_{i,j}^I = s_{i,j}^T = [\mathbf{z}_i^I]_{[\text{CLS}]}^\top [\mathbf{z}_j^T]_{[\text{SEP}]}$, where $[\mathbf{z}_i^I]_{[\text{CLS}]}$ denotes the feature vector of the [CLS] token of the i -th image and $[\mathbf{z}_j^T]_{[\text{SEP}]}$ denotes the feature vector of the [SEP] token of the j -th text. Since Swin Transformer has no [CLS] token, we use the average pooling on the features of all patch tokens to represent it.

Token-wise Similarity. In FILIP [53], the similarity is computed based on a finer-grained interaction between the image patches and textual tokens, which also brings good alignment and learns meaningful fine-grained features with promising localization ability. For i -th image, each visual token $[\mathbf{z}_i^I]_k$ in it computes a similarity with all non-padded textual tokens of the j -th text. Then the maximum one is used to represent the token-wise similarity between this visual token and the j -th text. Finally, we regard the average token-wise maximum similarity of all non-padded tokens in this i -th image as

the cross-modal similarity $s_{i,j}^I = \frac{1}{n_1} \sum_{k=1}^{n_1} [z_i^I]_k^\top [z_j^T]_{m_k^I}$, where $m_k^I = \arg \max_{0 \leq r < n_2} [z_i^I]_k^\top [z_j^T]_r$. The similarity of a text to an image can be computed in the same way, except that we exclude the [CLS], [SEP], and all padding tokens as in FILIP [53].

Reduced-token Interaction. Using the token-wise similarity introduces a large amount of computation. The computation cost is about $2 \times n_1 \times n_2$ times more than that of global similarity. The number of visual tokens n_1 is normally predefined while the number of textual tokens n_2 depends on the text input. To reduce the computation cost of token-wise similarity, an efficient way is to decrease the number of tokens involved in similarity calculation and we call this reduced-token interaction.

In this paper, we propose a learnable token reduction layer on top of visual features output by the image encoder. The workflow of this layer is described in the right part of Figure 1. Since the number of visual tokens is usually much larger than that of textual tokens, e.g., there are $16 \times 16 + 1 = 257$ visual tokens and 32 textual tokens for CLIP_{ViT-L}, visual tokens are more necessary to be decreased for efficiency. Denoting the visual tokens of an image sample as $z^I \in \mathbb{R}^{n_1 \times d}$, we aim to get a new $Z^I = f(z^I) \in \mathbb{R}^{n' \times d}$ in which f denotes the function of token reduction and n' denotes the reduced token number. Finally, z^I is replaced by Z^I to calculate the token-wise similarity. In general, given the output number of tokens n' , the k -th visual token $Z_k^I \in \mathbb{R}^d$ can be formulated by: $Z_k^I = \text{AvgPool}(\text{Conv}_k(z^I) \odot z^I)$, $k \in \{1, 2, \dots, n'\}$ where \odot represents Hadamard product. Firstly, $z_k^I \in \mathbb{R}^{n_1 \times d}$ is reshaped to $z_k^I \in \mathbb{R}^{H \times W \times d}$ in which H and W respectively represent the vertical and horizontal numbers of visual tokens. Then, the k -th attention map is computed via $\text{Conv}_k : \mathbb{R}^{H \times W \times d} \rightarrow \mathbb{R}^{H \times W \times 1}$ which is implemented using two convolutional layers. We share the weight of Conv_k across all k tokens. Finally, a spatial global average pooling $\text{AvgPool} : \mathbb{R}^{H \times W \times d} \rightarrow \mathbb{R}^d$ is used to get the final k -th visual token.

Locked-image Text tuning. LiT-tuning [57] proposes that a locked pre-trained image encoder with an unlocked text encoder works well in contrastive learning. We extend this idea to cross-lingual data sources and try to align a locked image encoder pre-trained on English data sources, e.g., CLIP [35] and FILIP [53], with a trainable Chinese text encoder. These existing pre-trained image encoders usually have a projection linear layer. In our method, we drop this linear layer and add a new linear trainable random-initialized projection layer, whose output dimension can be adjusted flexibly. Experiment results shown in Section 5.4 confirm its effectiveness.

5 Wukong Chinese Benchmarks

5.1 Experimental Setup

Following the existing VLP models, e.g., CLIP [35] and ALIGN [14], we employ a dual-encoder architecture as illustrated in Figure 1. We have three variations of pretraining Chinese models: global similarity (CLIP-style); token-wise similarity (FILIP-style) and token-wise similarity with token reduction layer (Wukong-style). For different types of visual encoders, we have ViT-B, ViT-L[8], and Swin-L[24]. We use the token-wise similarity with our proposed reduced-token interaction for Wukong-style models. For the dimension of the common multi-modal space, all the FILIP-style and Wukong-style models are set to 256 and CLIP-style models are set following the original CLIP checkpoints. Models are trained using LiT-tuning [57], since they achieve relatively better results as shown in Section 5.4. In terms of pre-loaded visual encoders, CLIP and FILIP models with ViT-B/32 or ViT-L/14 are used. Swin-L pre-trained on ImageNet-22K with 224×224 image resolution is used for Swin Transformer based models, e.g., CLIP_{Swin-L}. Detailed training settings are in the appendix.

5.2 Zero-shot Image Classification

We evaluate our models for the zero-shot classification task on 10 datasets whose class labels are translated from English. To make the evaluation results more reliable, the translation process is done with a machine translator and verified by human experts. The Chinese annotations of these datasets are released for future evaluation by the research community. Also, we evaluate BriVL [13], another multi-modal pre-training model for Chinese, on these datasets for zero-shot classification. The implementation code and pre-trained model weights of BriVL are both from its [homepage](#).

Prompt Ensemble. Text prompts are often used as a class label augmentation to achieve a better performance in the zero-shot image classification task [35, 53]. For simplicity, instead of designing prompts manually, we provide a set of 80 text prompts which are originally used on ImageNet by CLIP and manually translate them into Chinese. We also release these Chinese prompts for future fair comparison in our community.

Table 4: Top-1 accuracy (%) of the zero-shot image classification benchmark. All the models are trained using 100-million Wukong dataset except for BriVL which is pre-trained using its own dataset. Results highlighted with **bold** mean the best within the same image encoder and those with underline represent the best among all methods.

| Model \ Dataset (CN) | Dataset (CN) | | | | | | | | | | |
|------------------------------|--------------|-------------|-------------|-------------|-------------|-------------|-------------|-------------|-------------|-------------|--------------|
| | CIFAR10 | CIFAR100 | Caltech101 | Caltech256 | DTD | Sports | Flowers | SUN397 | EuroSAT | ImageNet | Average |
| BriVL [13] | 72.3 | 35.9 | 72.0 | 58.0 | 18.8 | 83.6 | 18.4 | 28.4 | 25.5 | 24.3 | 43.72 |
| CLIP _{ViT-B} [35] | 89.4 | 62.5 | 89.2 | 82.7 | 36.2 | 93.1 | 52.6 | 55.8 | 25.7 | 47.7 | 63.49 |
| FILIP _{ViT-B} [53] | 87.0 | 53.3 | 83.1 | 71.0 | 28.9 | 91.2 | 48.8 | 50.0 | 29.5 | 38.1 | 58.09 |
| Wukong _{ViT-B} | 87.1 | 62.6 | 89.1 | 82.3 | 37.3 | 95.6 | 64.8 | 56.0 | 32.6 | 49.1 | 65.65 |
| CLIP _{ViT-L} [35] | 94.1 | 71.3 | 91.9 | 89.0 | 45.4 | 98.7 | 72.3 | 62.6 | 42.8 | 57.9 | 72.60 |
| FILIP _{ViT-L} [53] | 90.6 | 66.3 | 89.9 | 86.2 | 46.4 | 97.8 | 69.4 | 60.2 | 25.5 | 54.0 | 68.63 |
| Wukong _{ViT-L} | 95.4 | 77.1 | 92.4 | 89.2 | 40.9 | 99.1 | 68.9 | 62.0 | 50.3 | 55.0 | 73.03 |
| CLIP _{Swin-L} [35] | 94.8 | 75.8 | 90.7 | 88.3 | 40.0 | 97.5 | 71.0 | 57.3 | 22.3 | 58.0 | 69.57 |
| FILIP _{Swin-L} [53] | 95.5 | 77.2 | 91.6 | 88.4 | 39.8 | 99.1 | 75.1 | 56.5 | 21.0 | 58.5 | 70.27 |
| Wukong _{Swin-L} | 95.3 | 76.8 | 89.8 | 87.1 | 33.7 | 97.8 | 76.9 | 56.3 | 19.3 | 58.2 | 69.12 |

Performance. The evaluation of zero-shot image classification on different datasets is illustrated in Table 4. In addition to our proposed models, i.e., Wukong_{ViT-B}, Wukong_{ViT-L}, and Wukong_{Swin-L}, we also evaluate other model architectures, i.e., CLIP and FILIP, with different image encoders as comparisons. These models are all pre-trained using our Wukong dataset except for BriVL which uses its own dataset. In comparison with models pre-trained using Wukong dataset, BriVL shows a significantly poor performance. This can be considered as the proof that Wukong dataset is effective for multi-modal pre-training. Besides, using the same ViT image encoder, either ViT-B or ViT-L, Wukong models perform quite well. In particular, Wukong_{ViT-L} achieves the highest average accuracy of 73.03% among all models. This indicates the superiority of our model architecture. However, our model trained with SwinT as the image encoder performs worse compared to others. The reason might be that patch merging in SwinT has already served a similar purpose in selecting and merging the important visual patch tokens. Therefore, our reduced-token interaction brings a negative impact. In summary, the zero-shot classification performances on various tasks show the effectiveness of our dataset and Wukong models.

5.3 Image-Text Retrieval

In this section, we evaluate our models on two sub-tasks, including image-to-text retrieval and text-to-image retrieval. In the image-to-text retrieval, the model retrieves a target text from a set of candidates given an image as query, or vice versa for the text-to-image retrieval. We benchmark our models on 6 different datasets, including Flickr8K-CN [20], Flickr30K-CN [18], COCO-CN [21], AIC-ICC [51], MUGE¹ and Wukong-Test.

Following common practices, we report Recall@K (recall of top K candidates) with $K = 1, 5, 10$ for both image-to-text and text-to-image retrieval on all datasets except for MUGE, which only has the text-to-image retrieval setting. The average Recall@K, i.e., Mean Recall (MR), is used for the final comparison. We report results on the test sets, except for MUGE and AIC-ICC where test sets are not released. For MUGE, we report results on the validation set, and for AIC-ICC, following the setting of WenLan 2.0 [9], we take the first 10K images along with their corresponding 50K pieces of texts from the validation set for testing.

Table 5 shows the benchmarks of zero-shot image-text retrieval using different models on multiple datasets. In general, models trained on Wukong dataset achieve a significantly better performance than BriVL [13], which demonstrates the effectiveness of our dataset. Besides, Wukong_{ViT-L} shows a competitive performance in comparison to other models. Therefore, we believe Wukong dataset can serve as a pre-training benchmark dataset with a wide coverage of concepts.

Table 6 shows the results of image-text retrieval task. Generally, Wukong_{ViT-L} achieves the best results among different model variants and datasets. Compared with baseline methods, on AIC-ICC, Wukong significantly outperforms WenLan 2.0 by around 12.9%, which was pre-trained on a larger dataset

¹<https://tianchi.aliyun.com/muge>

Table 5: Benchmarks of zero-shot image-text retrieval. The top-3 performance values are highlighted with **bold**, underline and *italic* respectively.

| Dataset | Method | Image-to-Text Retrieval | | | Text-to-Image Retrieval | | | MR |
|--------------|-----------------------------|-------------------------|------|------|-------------------------|------|------|-------------|
| | | R@1 | R@5 | R@10 | R@1 | R@5 | R@10 | |
| Flickr8K-CN | BriVL [13] | 13.4 | 31.2 | 40.7 | 8.0 | 20.7 | 29.5 | 23.9 |
| | CLIP _{ViT-B} | 59.5 | 86.2 | 93.4 | 44.2 | 71.2 | 82.0 | 72.7 |
| | CLIP _{ViT-L} [35] | 65.4 | 89.2 | 95.4 | 50.5 | 77.0 | 85.7 | <u>77.2</u> |
| | CLIP _{Swin-L} | 56.0 | 83.2 | 92.4 | 38.6 | 67.0 | 78.2 | 69.2 |
| | FILIP _{ViT-B} | 37.2 | 65.9 | 75.2 | 24.0 | 50.0 | 62.4 | 52.5 |
| | FILIP _{ViT-L} [53] | 70.0 | 91.6 | 96.6 | 53.5 | 79.3 | 87.9 | 79.8 |
| | FILIP _{Swin-L} | 52.4 | 78.0 | 87.2 | 41.2 | 68.5 | 79.1 | 67.7 |
| | Wukong _{ViT-B} | 55.4 | 82.3 | 90.0 | 43.2 | 71.3 | 81.3 | 70.6 |
| | Wukong _{ViT-L} | 61.4 | 86.2 | 93.6 | 46.0 | 74.5 | 84.5 | <u>74.4</u> |
| | Wukong _{Swin-L} | 47.2 | 78.8 | 87.6 | 36.6 | 64.8 | 76.2 | 65.2 |
| Flickr30K-CN | BriVL [13] | 17.7 | 42.3 | 54.3 | 10.3 | 27.5 | 37.9 | 31.7 |
| | CLIP _{ViT-B} | 72.2 | 92.0 | 96.4 | 47.2 | 74.1 | 82.9 | 77.5 |
| | CLIP _{ViT-L} [35] | 75.0 | 94.5 | 97.7 | 51.8 | 78.6 | 85.9 | <u>80.6</u> |
| | CLIP _{Swin-L} | 64.3 | 89.3 | 94.3 | 41.2 | 69.7 | 80.2 | 73.2 |
| | FILIP _{ViT-B} | 44.2 | 73.7 | 83.3 | 28.7 | 55.9 | 67.1 | 58.8 |
| | FILIP _{ViT-L} [53] | 78.9 | 96.2 | 98.1 | 55.7 | 81.2 | 87.9 | 83.0 |
| | FILIP _{Swin-L} | 65.8 | 89.2 | 95.0 | 44.6 | 72.2 | 81.2 | 74.7 |
| | Wukong _{ViT-B} | 66.2 | 88.7 | 94.3 | 45.7 | 73.8 | 82.2 | 75.1 |
| | Wukong _{ViT-L} | 76.1 | 94.8 | 97.5 | 51.7 | 78.9 | 86.3 | <u>80.9</u> |
| | Wukong _{Swin-L} | 58.7 | 86.7 | 92.7 | 40.9 | 68.0 | 78.4 | 70.9 |
| COCO-CN | BriVL [13] | 17.1 | 41.7 | 57.5 | 14.8 | 39.0 | 54.2 | 37.4 |
| | CLIP _{ViT-B} | 52.8 | 79.6 | 88.9 | 48.7 | 79.4 | 88.5 | <u>73.0</u> |
| | CLIP _{ViT-L} [35] | 51.0 | 80.0 | 89.7 | 48.7 | 76.8 | 86.4 | 72.1 |
| | CLIP _{Swin-L} | 50.5 | 79.2 | 88.2 | 46.7 | 78.1 | 87.7 | 71.7 |
| | FILIP _{ViT-B} | 37.8 | 66.4 | 77.9 | 37.5 | 68.1 | 83.0 | 61.8 |
| | FILIP _{ViT-L} [53] | 56.9 | 82.4 | 90.9 | 52.7 | 79.9 | 88.6 | 75.2 |
| | FILIP _{Swin-L} | 48.6 | 77.3 | 88.3 | 50.5 | 79.2 | 88.6 | 72.1 |
| | Wukong _{ViT-B} | 48.3 | 77.8 | 88.8 | 49.2 | 79.4 | 87.9 | 71.9 |
| | Wukong _{ViT-L} | 55.2 | 81.0 | 90.6 | 53.4 | 80.2 | 90.1 | <u>75.1</u> |
| | Wukong _{Swin-L} | 47.3 | 78.0 | 88.3 | 46.4 | 77.0 | 87.6 | 70.8 |
| MUGE | BriVL [13] | - | - | - | 12.7 | 30.9 | 41.8 | 28.5 |
| | CLIP _{ViT-B} | - | - | - | 37.3 | 64.2 | 73.9 | <u>58.5</u> |
| | CLIP _{ViT-L} [35] | - | - | - | 43.3 | 69.2 | 78.4 | 63.6 |
| | CLIP _{Swin-L} | - | - | - | 35.2 | 62.2 | 73.2 | 56.9 |
| | FILIP _{ViT-B} | - | - | - | 22.4 | 46.6 | 58.5 | 42.5 |
| | FILIP _{ViT-L} [53] | - | - | - | 37.6 | 63.4 | 73.6 | 58.2 |
| | FILIP _{Swin-L} | - | - | - | 36.2 | 61.1 | 71.5 | 56.3 |
| | Wukong _{ViT-B} | - | - | - | 33.4 | 59.3 | 69.7 | 54.1 |
| | Wukong _{ViT-L} | - | - | - | 42.7 | 69.0 | 78.0 | <u>63.2</u> |
| | Wukong _{Swin-L} | - | - | - | 34.5 | 60.6 | 71.2 | 55.5 |

consisting of 650 million image-text pairs. For the COCO-CN dataset, our Wukong models also achieve comparable performance to state-of-the-art methods. For Wukong-Test, CLIP_{ViT-L} achieves the best result (89.6%) so far. It shows that models with global similarity is particularly effective when massively trained on in-domain Wukong train set. However, it lacks a bit of generalization when finetuned on other out-of-domain datasets such as AIC-ICC and MUGE. Overall, experimental results demonstrate the capabilities of our pre-trained models.

5.4 Ablations and Findings

Locked-image Text Tuning. To evaluate the effectiveness of LiT-tuning, we take Wukong_{ViT-B} as an example model for a detailed investigation. We train two models using the same experimental settings as mentioned above, apart from that one model is trained with a locked image encoder but the other is not locked. As shown in Figure 2, the model using LiT-tuning method shows a slower trend of loss decrease during training. We believe the unlocked image encoder contributes to reduce the training loss and find the local optima efficiently. However, the validation accuracy of LiT-tuning model remains higher than the other in almost every iteration, which demonstrates a better generalization.

Visualization. In addition, we present the visualization of word-patch alignment in the appendix, which evidences the effectiveness of cross-modal token-wise similarity even in the LiT-tuning setting. We apply the same visualization method from FILIP [53], to align textual tokens and image patch tokens from FILIP_{ViT-L} and FILIP_{Swin-L}. We find that both models can predict image patches of the target object, and more details are shown in the appendix. Given this promising capability of aligning words and patches, our released models offer a potential solution for image object localization.

Table 6: Benchmarks of fine-tuned image-text retrieval on different datasets. The top-3 performance values are highlighted with **bold**, underline and *italic* respectively.

| Dataset | Method | Image-to-Text Retrieval | | | Text-to-Image Retrieval | | | MR |
|--------------------------|-----------------------------|-------------------------|------|------|-------------------------|------|-------------|-------------|
| | | R@1 | R@5 | R@10 | R@1 | R@5 | R@10 | |
| Flickr8K-CN | CLIP _{ViT-B} | 77.7 | 94.7 | 98.1 | 61.2 | 86.8 | 93.2 | 85.3 |
| | CLIP _{ViT-L} [35] | 81.4 | 96.9 | 99.0 | 67.4 | 91.0 | 95.7 | <u>88.6</u> |
| | CLIP _{Swin-L} | 77.3 | 94.9 | 98.2 | 59.3 | 86.0 | 92.9 | 84.8 |
| | FILIP _{ViT-B} | 52.6 | 81.5 | 90.2 | 46.4 | 77.0 | 86.8 | 72.4 |
| | FILIP _{ViT-L} [53] | 80.8 | 94.8 | 98.3 | 68.5 | 90.5 | 95.2 | <u>88.0</u> |
| | FILIP _{Swin-L} | 77.6 | 94.4 | 97.7 | 61.5 | 86.5 | 93.0 | 85.1 |
| | Wukong _{ViT-B} | 71.7 | 91.5 | 96.6 | 58.4 | 85.4 | 92.0 | 82.6 |
| | Wukong _{ViT-L} | 83.3 | 97.3 | 99.5 | 70.1 | 91.9 | 96.4 | 89.7 |
| Wukong _{Swin-L} | 74.9 | 93.6 | 97.8 | 57.9 | 85.1 | 92.6 | 83.6 | |
| Flickr30K-CN | CLIP _{ViT-B} | 87.1 | 97.7 | 98.8 | 69.0 | 90.3 | 95.0 | 89.7 |
| | CLIP _{ViT-L} [35] | 91.6 | 99.1 | 99.7 | 77.3 | 94.4 | 97.2 | <u>93.2</u> |
| | CLIP _{Swin-L} | 85.8 | 97.1 | 99.0 | 67.4 | 90.3 | 94.9 | 89.1 |
| | FILIP _{ViT-B} | 72.1 | 91.3 | 95.8 | 57.5 | 84.3 | 90.6 | 81.9 |
| | FILIP _{ViT-L} [53] | 90.6 | 98.8 | 99.6 | 76.9 | 94.9 | 97.4 | <u>93.0</u> |
| | FILIP _{Swin-L} | 86.0 | 97.5 | 99.1 | 70.9 | 91.3 | 95.3 | 90.0 |
| | Wukong _{ViT-B} | 83.9 | 97.6 | 99.0 | 67.6 | 89.6 | 94.2 | 88.7 |
| | Wukong _{ViT-L} | 92.7 | 99.1 | 99.6 | 77.4 | 94.5 | 97.0 | 93.4 |
| | Wukong _{Swin-L} | 86.2 | 98.1 | 99.4 | 67.4 | 89.9 | 94.5 | 89.3 |
| COCO-CN | EmbN [49] | - | - | - | - | - | - | 73.2 |
| | PARALLEL-EmbN [10] | - | - | - | - | - | - | 76.0 |
| | S-LIWE [50] | - | - | - | - | - | - | 73.6 |
| | M ³ P [29] | - | - | - | - | - | - | 86.2 |
| | UNITER [3] | - | - | - | - | - | - | 87.3 |
| | LightningDOT [47] | - | - | - | - | - | - | <u>88.4</u> |
| | UC ² [59] | - | - | - | - | - | - | 89.8 |
| | CLIP _{ViT-B} | 68.7 | 93.6 | 97.5 | 68.9 | 93.3 | 97.3 | 86.6 |
| | CLIP _{ViT-L} [35] | 68.3 | 93.0 | 97.3 | 70.1 | 92.2 | 96.4 | 86.2 |
| | CLIP _{Swin-L} | 68.0 | 92.8 | 97.3 | 66.7 | 91.5 | 96.3 | 85.4 |
| | FILIP _{ViT-B} | 52.7 | 81.3 | 88.3 | 56.2 | 86.8 | 94.3 | 76.6 |
| | FILIP _{ViT-L} [53] | 69.1 | 91.3 | 96.9 | 72.2 | 92.4 | 97.2 | 86.5 |
| | FILIP _{Swin-L} | 68.3 | 93.9 | 97.1 | 69.9 | 93.3 | 97.6 | 86.7 |
| Wukong _{ViT-B} | 65.8 | 90.3 | 96.6 | 67.0 | 91.4 | 96.7 | 84.6 | |
| Wukong _{ViT-L} | 73.3 | 94.0 | 98.0 | 74.0 | 94.4 | 98.1 | <u>88.6</u> | |
| Wukong _{Swin-L} | 67.4 | 92.4 | 97.5 | 66.0 | 92.6 | 97.1 | 85.5 | |
| AIC-ICC | WenLan 2.0 [9] | 45.6 | 68.0 | 76.3 | 34.1 | 58.9 | 69.1 | 58.7 |
| | CLIP _{ViT-B} | 50.5 | 73.0 | 80.2 | 38.1 | 63.7 | 73.3 | 63.1 |
| | CLIP _{ViT-L} [35] | 59.1 | 79.5 | 85.2 | 46.2 | 70.7 | 78.6 | <u>69.9</u> |
| | CLIP _{Swin-L} | 50.5 | 73.5 | 81.2 | 37.3 | 62.8 | 72.7 | 63.0 |
| | FILIP _{ViT-B} | 42.5 | 67.2 | 76.0 | 32.9 | 58.4 | 68.8 | 57.6 |
| | FILIP _{ViT-L} [53] | 54.1 | 75.8 | 82.8 | 44.9 | 69.0 | 77.5 | <u>67.4</u> |
| | FILIP _{Swin-L} | 53.1 | 74.8 | 82.0 | 41.1 | 65.7 | 74.7 | 65.2 |
| | Wukong _{ViT-B} | 47.5 | 70.6 | 78.6 | 36.7 | 56.7 | 71.7 | 57.0 |
| | Wukong _{ViT-L} | 61.6 | 80.5 | 86.1 | 48.6 | 72.5 | 80.2 | 71.6 |
| Wukong _{Swin-L} | 50.9 | 73.6 | 81.5 | 38.6 | 64.1 | 73.6 | 63.7 | |
| MUGE | CLIP _{ViT-B} | - | - | - | 43.5 | 71.7 | 80.6 | 65.3 |
| | CLIP _{ViT-L} [35] | - | - | - | 50.1 | 76.9 | 84.9 | <u>70.6</u> |
| | CLIP _{Swin-L} | - | - | - | 45.3 | 72.1 | 81.1 | <u>66.2</u> |
| | FILIP _{ViT-B} | - | - | - | 30.6 | 58.2 | 70.2 | 53.0 |
| | FILIP _{ViT-L} [53] | - | - | - | 43.5 | 71.5 | 80.9 | 65.3 |
| | FILIP _{Swin-L} | - | - | - | 44.0 | 71.4 | 81.2 | 65.5 |
| | Wukong _{ViT-B} | - | - | - | 39.2 | 66.9 | 77.4 | 61.2 |
| | Wukong _{ViT-L} | - | - | - | 52.7 | 77.9 | 85.6 | 72.1 |
| Wukong _{Swin-L} | - | - | - | 43.8 | 71.9 | 81.7 | 65.8 | |
| Wukong-Test | CLIP _{ViT-B} | 58.3 | 88.2 | 94.1 | 53.1 | 85.4 | 92.6 | <u>78.6</u> |
| | CLIP _{ViT-L} [35] | 72.8 | 98.2 | 99.8 | 68.9 | 98.0 | 99.8 | 89.6 |
| | CLIP _{Swin-L} | 56.0 | 86.1 | 92.5 | 51.0 | 83.4 | 90.9 | 76.7 |
| | FILIP _{ViT-B} | 30.3 | 57.6 | 66.9 | 20.2 | 47.5 | 60.3 | 47.1 |
| | FILIP _{ViT-L} [53] | 53.0 | 85.3 | 92.7 | 50.4 | 84.1 | 92.0 | 76.3 |
| | FILIP _{Swin-L} | 51.0 | 81.6 | 88.9 | 45.2 | 77.9 | 87.0 | 71.9 |
| | Wukong _{ViT-B} | 50.5 | 82.7 | 90.5 | 47.1 | 80.1 | 88.9 | 73.3 |
| | Wukong _{ViT-L} | 68.0 | 94.4 | 98.0 | 63.8 | 93.0 | 97.3 | <u>85.8</u> |
| Wukong _{Swin-L} | 53.1 | 85.4 | 92.2 | 47.8 | 81.6 | 89.7 | 75.0 | |

Tokenization for Chinese. We investigate the influence of the word segmentation technique on Chinese VLP models. Comparing the common character-grained tokenization, word-grained tokenization with a larger vocabulary (65,328) is also adopted. Results show that the model using character-grained tokenization achieves better performance. The detailed comparison is shown in

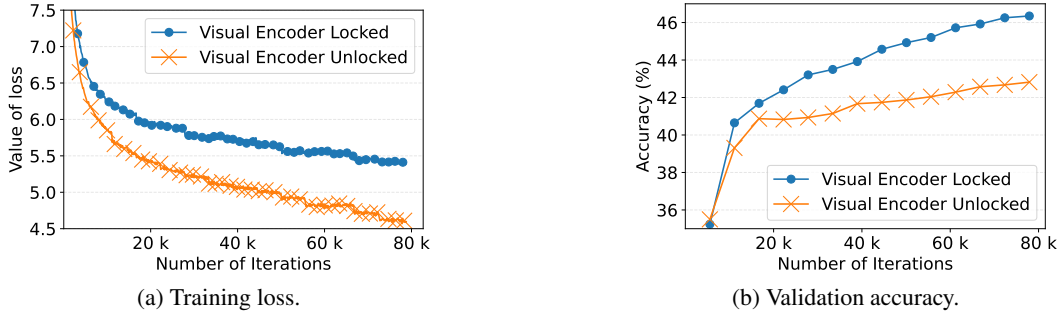


Figure 2: In comparison with the model trained with an unlocked image encoder, though the loss decreases slower when the image encoder is locked, the accuracy of evaluation remains a higher level.

the appendix. Since a Chinese word often contains more than one character, the character-grained tokens are more fine-grained than word-grained. One example is that the word “蜂鸟”(hummingbird) consists of two characters: “蜂”(bee) and “鸟”(bird). Therefore, we believe it is more effective for our models to learn deep semantic token-wise similarity between an image patch and its paired fine-grained textual tokens, in such a contrastive learning manner.

6 Conclusion

In this work, we build a large-scale Chinese vision-language dataset called Wukong. To the best of our knowledge, it is the first hundred-million level dataset designed for the Chinese language and it paves the way for future research on Chinese cross-modal pre-training. Meanwhile, using this dataset, we propose three Chinese VLP models, i.e., Wukong_{ViT-B}, Wukong_{ViT-L}, and Wukong_{Swin-L}. Our pre-trained Wukong_{ViT-L} achieves state-of-the-art performance on Chinese benchmarks such as zero-shot image classification and image-text retrieval tasks. In the future, we plan to explore more solutions to train multilingual cross-modal models with the Wukong dataset. Meanwhile, more downstream tasks, in addition to image classification and retrieval, are worth sufficient evaluation. Also, Wukong-based applications such as image search engines and visual question answering will be further explored in future work.

References

- [1] T. B. Brown, B. Mann, N. Ryder, M. Subbiah, J. Kaplan, P. Dhariwal, A. Neelakantan, P. Shyam, G. Sastry, A. Askell, et al. Language models are few-shot learners. In *Advances in neural information processing systems*, 2020.
- [2] S. Changpinyo, P. Sharma, N. Ding, and R. Soricut. Conceptual 12M: Pushing web-scale image-text pre-training to recognize long-tail visual concepts. In *IEEE/CVF Conference on Computer Vision and Pattern Recognition*, 2021.
- [3] Y.-C. Chen, L. Li, L. Yu, A. El Kholy, F. Ahmed, Z. Gan, Y. Cheng, and J. Liu. Uniter: Universal image-text representation learning. In *European conference on computer vision*, pages 104–120. Springer, 2020.
- [4] E. D. Cubuk, B. Zoph, D. Mane, V. Vasudevan, and Q. V. Le. Autoaugment: Learning augmentation strategies from data. In *Proceedings of the IEEE/CVF Conference on Computer Vision and Pattern Recognition*, pages 113–123, 2019.
- [5] J. Deng, W. Dong, R. Socher, L.-J. Li, K. Li, and L. Fei-Fei. Imagenet: A large-scale hierarchical image database. In *2009 IEEE conference on computer vision and pattern recognition*, pages 248–255. Ieee, 2009.
- [6] K. Desai, G. Kaul, Z. Aysola, and J. Johnson. Redcaps: Web-curated image-text data created by the people, for the people. *arXiv preprint arXiv:2111.11431*, 2021.
- [7] J. Devlin, M.-W. Chang, K. Lee, and K. Toutanova. Bert: Pre-training of deep bidirectional transformers for language understanding. In *Annual Conference of the North American Chapter of the Association for Computational Linguistics*, 2019.
- [8] A. Dosovitskiy, L. Beyer, A. Kolesnikov, D. Weissenborn, X. Zhai, T. Unterthiner, M. Dehghani, M. Minderoeder, G. Heigold, S. Gelly, et al. An image is worth 16x16 words: Transformers for image recognition at scale. In *International Conference on Learning Representations*, 2020.
- [9] N. Fei, Z. Lu, Y. Gao, G. Yang, Y. Huo, J. Wen, H. Lu, R. Song, X. Gao, T. Xiang, et al. Wenlan 2.0: Make ai imagine via a multimodal foundation model. *arXiv preprint arXiv:2110.14378*, 2021.
- [10] S. Gella, R. Sennrich, F. Keller, and M. Lapata. Image pivoting for learning multilingual multimodal representations. *arXiv preprint arXiv:1707.07601*, 2017.
- [11] Y. Goyal, T. Khot, D. Summers-Stay, D. Batra, and D. Parikh. Making the v in vqa matter: Elevating the role of image understanding in visual question answering. In *Proceedings of the IEEE conference on computer vision and pattern recognition*, pages 6904–6913, 2017.
- [12] K. He, H. Fan, Y. Wu, S. Xie, and R. Girshick. Momentum contrast for unsupervised visual representation learning. In *Proceedings of the IEEE/CVF conference on computer vision and pattern recognition*, pages 9729–9738, 2020.
- [13] Y. Huo, M. Zhang, G. Liu, H. Lu, Y. Gao, G. Yang, J. Wen, H. Zhang, B. Xu, W. Zheng, et al. Wenlan: Bridging vision and language by large-scale multi-modal pre-training. *arXiv preprint arXiv:2103.06561*, 2021.
- [14] C. Jia, Y. Yang, Y. Xia, Y.-T. Chen, Z. Parekh, H. Pham, Q. V. Le, Y. Sung, Z. Li, and T. Duerig. Scaling up visual and vision-language representation learning with noisy text supervision. In *International Conference on Machine Learning*, 2021.
- [15] W. Kim, B. Son, and I. Kim. Vilt: Vision-and-language transformer without convolution or region supervision. In *International Conference on Machine Learning*, 2021.
- [16] V. V. Kindratenko, J. J. Enos, G. Shi, M. T. Showerman, G. W. Arnold, J. E. Stone, J. C. Phillips, and W.-m. Hwu. Gpu clusters for high-performance computing. In *2009 IEEE International Conference on Cluster Computing and Workshops*, pages 1–8. IEEE, 2009.
- [17] R. Krishna, Y. Zhu, O. Groth, J. Johnson, K. Hata, J. Kravitz, S. Chen, Y. Kalantidis, L.-J. Li, D. A. Shamma, et al. Visual genome: Connecting language and vision using crowdsourced dense image annotations. *arXiv preprint arXiv:1602.07332*, 2016.
- [18] W. Lan, X. Li, and J. Dong. Fluency-guided cross-lingual image captioning. In *Proceedings of the 25th ACM international conference on Multimedia*, pages 1549–1557, 2017.
- [19] L. H. Li, M. Yatskar, D. Yin, C.-J. Hsieh, and K.-W. Chang. Visualbert: A simple and performant baseline for vision and language. *arXiv preprint arXiv:1908.03557*, 2019.
- [20] X. Li, W. Lan, J. Dong, and H. Liu. Adding chinese captions to images. In *Proceedings of the 2016 ACM on international conference on multimedia retrieval*, pages 271–275, 2016.
- [21] X. Li, C. Xu, X. Wang, W. Lan, Z. Jia, G. Yang, and J. Xu. Coco-cn for cross-lingual image tagging, captioning, and retrieval. *IEEE Transactions on Multimedia*, 21(9):2347–2360, 2019.

- [22] J. Lin, R. Men, A. Yang, C. Zhou, M. Ding, Y. Zhang, P. Wang, A. Wang, L. Jiang, X. Jia, et al. M6: A chinese multimodal pretrainer. *arXiv preprint arXiv:2103.00823*, 2021.
- [23] T.-Y. Lin, M. Maire, S. Belongie, J. Hays, P. Perona, D. Ramanan, P. Dollár, and C. L. Zitnick. Microsoft coco: Common objects in context. In *European conference on computer vision*, pages 740–755. Springer, 2014.
- [24] Z. Liu, Y. Lin, Y. Cao, H. Hu, Y. Wei, Z. Zhang, S. Lin, and B. Guo. Swin transformer: Hierarchical vision transformer using shifted windows. In *Proceedings of the IEEE/CVF International Conference on Computer Vision*, pages 10012–10022, 2021.
- [25] I. Loshchilov and F. Hutter. Sgdr: Stochastic gradient descent with warm restarts. *arXiv preprint arXiv:1608.03983*, 2016.
- [26] J. Lu, D. Batra, D. Parikh, and S. Lee. Vilbert: pretraining task-agnostic visiolinguistic representations for vision-and-language tasks. In *International Conference on Neural Information Processing Systems*, pages 13–23, 2019.
- [27] D. Mahajan, R. Girshick, V. Ramanathan, K. He, M. Paluri, Y. Li, A. Bharambe, and L. Van Der Maaten. Exploring the limits of weakly supervised pretraining. In *Proceedings of the European conference on computer vision (ECCV)*, pages 181–196, 2018.
- [28] D. Narayanan, M. Shoenybi, J. Casper, P. LeGresley, M. Patwary, V. A. Korthikanti, D. Vainbrand, P. Kashinkunti, J. Bernauer, B. Catanzaro, et al. Efficient large-scale language model training on gpu clusters. *arXiv preprint arXiv:2104.04473*, 2021.
- [29] M. Ni, H. Huang, L. Su, E. Cui, T. Bharti, L. Wang, D. Zhang, and N. Duan. M3p: Learning universal representations via multitask multilingual multimodal pre-training. In *Proceedings of the IEEE/CVF Conference on Computer Vision and Pattern Recognition*, pages 3977–3986, 2021.
- [30] V. Ordonez, G. Kulkarni, and T. Berg. Im2text: Describing images using 1 million captioned photographs. In J. Shawe-Taylor, R. Zemel, P. Bartlett, F. Pereira, and K. Q. Weinberger, editors, *Advances in Neural Information Processing Systems*, volume 24. Curran Associates, Inc., 2011.
- [31] V. Ordonez, G. Kulkarni, and T. Berg. Im2text: Describing images using 1 million captioned photographs. *Advances in neural information processing systems*, 24, 2011.
- [32] Z. Parekh, J. Baldridge, D. Cer, A. Waters, and Y. Yang. Crisscrossed captions: Extended intramodal and intermodal semantic similarity judgments for ms-coco. *arXiv preprint arXiv:2004.15020*, 2020.
- [33] T. Pires, E. Schlinger, and D. Garrette. How multilingual is multilingual bert? *arXiv preprint arXiv:1906.01502*, 2019.
- [34] B. A. Plummer, L. Wang, C. M. Cervantes, J. C. Caicedo, J. Hockenmaier, and S. Lazebnik. Flickr30k entities: Collecting region-to-phrase correspondences for richer image-to-sentence models. In *Proceedings of the IEEE international conference on computer vision*, pages 2641–2649, 2015.
- [35] A. Radford, J. W. Kim, C. Hallacy, A. Ramesh, G. Goh, S. Agarwal, G. Sastry, A. Askell, P. Mishkin, J. Clark, et al. Learning transferable visual models from natural language supervision. In *International Conference on Machine Learning*, pages 8748–8763. PMLR, 2021.
- [36] C. Raffel, N. Shazeer, A. Roberts, K. Lee, S. Narang, M. Matena, Y. Zhou, W. Li, and P. J. Liu. Exploring the limits of transfer learning with a unified text-to-text transformer. *Journal of Machine Learning Research*, 21:1–67, 2020.
- [37] S. Rajbhandari, J. Rasley, O. Ruwase, and Y. He. Zero: Memory optimizations toward training trillion parameter models. In *SC20: International Conference for High Performance Computing, Networking, Storage and Analysis*, pages 1–16. IEEE, 2020.
- [38] J. Rasley, S. Rajbhandari, O. Ruwase, and Y. He. Deepspeed: System optimizations enable training deep learning models with over 100 billion parameters. In *Proceedings of the 26th ACM SIGKDD International Conference on Knowledge Discovery & Data Mining*, pages 3505–3506, 2020.
- [39] C. Riquelme, J. Puigcerver, B. Mustafa, M. Neumann, R. Jenatton, A. Susano Pinto, D. Keysers, and N. Houlsby. Scaling vision with sparse mixture of experts. *Advances in Neural Information Processing Systems*, 34, 2021.
- [40] M. Ryoo, A. Piergiovanni, A. Arnab, M. Dehghani, and A. Angelova. Tokenlearner: Adaptive space-time tokenization for videos. *Advances in Neural Information Processing Systems*, 34, 2021.
- [41] C. Schuhmann, R. Vencu, R. Beaumont, R. Kaczmarczyk, C. Mullis, A. Katta, T. Coombes, J. Jitsev, and A. Komatsuzaki. Laion-400m: Open dataset of clip-filtered 400 million image-text pairs. *arXiv preprint arXiv:2111.02114*, 2021.
- [42] P. Sharma, N. Ding, S. Goodman, and R. Soricut. Conceptual captions: A cleaned, hypernymed, image alt-text dataset for automatic image captioning. In *Annual Meeting of the Association for Computational Linguistics (Volume 1: Long Papers)*, pages 2556–2565, 2018.

- [43] Y. Song, S. Shi, J. Li, and H. Zhang. Directional skip-gram: Explicitly distinguishing left and right context for word embeddings. In *Proceedings of the 2018 Conference of the North American Chapter of the Association for Computational Linguistics: Human Language Technologies, Volume 2 (Short Papers)*, pages 175–180, 2018.
- [44] K. Srinivasan, K. Raman, J. Chen, M. Bendersky, and M. Najork. Wit: Wikipedia-based image text dataset for multimodal multilingual machine learning. In *Proceedings of the 44th International ACM SIGIR Conference on Research and Development in Information Retrieval*, pages 2443–2449, 2021.
- [45] J. A. Stuart and J. D. Owens. Multi-gpu mapreduce on gpu clusters. In *2011 IEEE International Parallel & Distributed Processing Symposium*, pages 1068–1079. IEEE, 2011.
- [46] C. Sun, A. Shrivastava, S. Singh, and A. Gupta. Revisiting unreasonable effectiveness of data in deep learning era. In *Proceedings of the IEEE international conference on computer vision*, pages 843–852, 2017.
- [47] S. Sun, Y.-C. Chen, L. Li, S. Wang, Y. Fang, and J. Liu. Lightningdot: Pre-training visual-semantic embeddings for real-time image-text retrieval. In *Proceedings of the 2021 Conference of the North American Chapter of the Association for Computational Linguistics: Human Language Technologies*, pages 982–997, 2021.
- [48] B. Thomee, D. A. Shamma, G. Friedland, B. Elizalde, K. Ni, D. Poland, D. Borth, and L.-J. Li. Yfcc100m: The new data in multimedia research. *Communications of the ACM*, 59(2):64–73, 2016.
- [49] L. Wang, Y. Li, J. Huang, and S. Lazebnik. Learning two-branch neural networks for image-text matching tasks. *IEEE Transactions on Pattern Analysis and Machine Intelligence*, 41(2):394–407, 2018.
- [50] J. Wehrmann, D. M. Souza, M. A. Lopes, and R. C. Barros. Language-agnostic visual-semantic embeddings. In *Proceedings of the IEEE/CVF International Conference on Computer Vision*, pages 5804–5813, 2019.
- [51] J. Wu, H. Zheng, B. Zhao, Y. Li, B. Yan, R. Liang, W. Wang, S. Zhou, G. Lin, Y. Fu, et al. Ai challenger: A large-scale dataset for going deeper in image understanding. *arXiv preprint arXiv:1711.06475*, 2017.
- [52] Y. Wu, M. Schuster, Z. Chen, Q. V. Le, M. Norouzi, W. Macherey, M. Krikun, Y. Cao, Q. Gao, K. Macherey, J. Klingner, A. Shah, M. Johnson, X. Liu, L. Kaiser, S. Gouws, Y. Kato, T. Kudo, H. Kazawa, K. Stevens, G. Kurian, N. Patil, W. Wang, C. Young, J. Smith, J. Riesa, A. Rudnick, O. Vinyals, G. Corrado, M. Hughes, and J. Dean. Google’s neural machine translation system: Bridging the gap between human and machine translation. *arXiv preprint arXiv:1609.08144*, 2016.
- [53] L. Yao, R. Huang, L. Hou, G. Lu, M. Niu, H. Xu, X. Liang, Z. Li, X. Jiang, and C. Xu. Filip: Fine-grained interactive language-image pre-training. In *ICLR*, 2022.
- [54] Y. You, J. Li, S. Reddi, J. Hseu, S. Kumar, S. Bhojanapalli, X. Song, J. Demmel, K. Keutzer, and C.-J. Hsieh. Large batch optimization for deep learning: Training bert in 76 minutes. In *International Conference on Learning Representations*, 2020.
- [55] P. Young, A. Lai, M. Hodosh, and J. Hockenmaier. From image descriptions to visual denotations: New similarity metrics for semantic inference over event descriptions. *Transactions of the Association for Computational Linguistics*, 2:67–78, 2014.
- [56] X. Zhai, A. Kolesnikov, N. Houlsby, and L. Beyer. Scaling vision transformers. *arXiv preprint arXiv:2106.04560*, 2021.
- [57] X. Zhai, X. Wang, B. Mustafa, A. Steiner, D. Keysers, A. Kolesnikov, and L. Beyer. Lit: Zero-shot transfer with locked-image text tuning. *arXiv preprint arXiv:2111.07991*, 2021.
- [58] X. Zhan, Y. Wu, X. Dong, Y. Wei, M. Lu, Y. Zhang, H. Xu, and X. Liang. Product1m: Towards weakly supervised instance-level product retrieval via cross-modal pretraining. In *International Conference on Computer Vision*, 2021.
- [59] M. Zhou, L. Zhou, S. Wang, Y. Cheng, L. Li, Z. Yu, and J. Liu. Uc2: Universal cross-lingual cross-modal vision-and-language pre-training. In *Proceedings of the IEEE/CVF Conference on Computer Vision and Pattern Recognition*, pages 4155–4165, 2021.

Appendix

A Examples in Wukong Dataset

Figure 3 shows some examples in our dataset. These image-text pairs involve many types of content, e.g., social news, sporting events, product introduction, et al. Therefore, our dataset is suitable for general-purpose multi-modal pre-training. Additionally, in Figure 4, we visualize the distribution of words (consisting of one or more tokens) in our dataset. We use the Chinese text segmentation



Figure 3: Examples of image-text pairs in Wukong dataset. A diverse range of concepts are included.



Figure 4: The word cloud generated with texts in Wukong dataset. For example, “月” means month; “日” is day; “做” is do and “一个” means one.

module *jieba*² to generate words and build this word cloud of our dataset. Additionally, for the topics or themes of the samples, Figure 5 shows the word frequency of nouns in our dataset. Naturally, a long tail distribution is followed and a wide range of concepts are covered.

B Experimental Setup

The experimental settings of our model variants are described in Table 7. For better generalization and data-efficiency, we employ Autoaugment [4] for image data augmentation that aims to build more image-text pairs. All of our models are trained using Nvidia V100 GPUs and Ascend cards. Specifically, Wukong_{VIT-B} is trained using 32 GPUs for 3 days, Wukong_{VIT-L} is trained using 32 GPUs for 10 days and Wukong_{Swin-L} is trained using 40 GPUs for 5 days. We use LAMB optimizer [54] and cosine learning rate schedule with a linear warmup [25]. Weight decay regularization is applied

²<https://github.com/fxsjy/jieba>

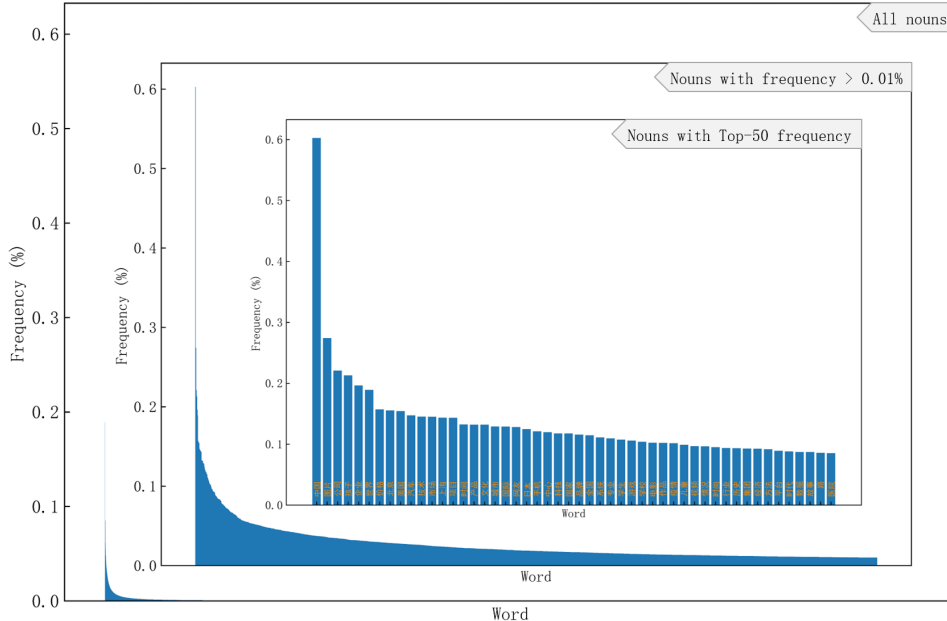


Figure 5: The word frequency of nouns in our dataset. A wide range of concepts are covered.

Table 7: Detailed settings of our model variants. The resolution of image is 224×224 and the length of text is 32.

| Model | Image encoder | Linear projected embeddings | Token reduction | Text encoder | | | #Parameters |
|--------------------------|---------------|-----------------------------|-----------------|--------------|--------|-------|-------------|
| | | | | #layers | #heads | width | |
| Wukong _{ViT-B} | ViT-B/32 | 256 | 12 | 12 | 8 | 512 | 136M |
| Wukong _{ViT-L} | ViT-L/14 | 256 | 24 | 12 | 12 | 768 | 404M |
| Wukong _{Swin-L} | Swin-L | 256 | 12 | 12 | 12 | 768 | 297M |

Table 8: Hyper-parameters used in model training.

| Initial Temperature | LAMB | | | Total Epochs |
|---------------------|-----------|-----------|------------|--------------|
| | β_1 | β_2 | ϵ | |
| 0.07 | 0.9 | 0.999 | 10^{-2} | 20 |

to all parameters except for bias, layer normalization, token embedding, positional embedding and temperature in the contrastive loss. The detailed hyper-parameters are shown in Table 8. In order to pick the optimal checkpoint out, ImageNet dataset [5] with translated class names is used for zero-shot validation.

C Supplementary Experiments

C.1 Tokenization for Chinese

Table 9 shows the comparison between using the character-grained and word-grained tokenization in our Wukong_{ViT-B} model. We use the python module *jieba* to do Chinese word segmentation to split Chinese text into words. All experimental settings remain the same except for the tokenization. Results show that Wukong_{ViT-B} achieve better performance than Wukong_{ViT-B-Word}. We believe the main reason is that the character-grained tokens are more fine-grained than word-grained, since a Chinese word often contains more than one character. Such character-grained method contributes to help models learn the deep semantic token-wise similarity between an image patch with its paired

Table 9: Comparison of character-grained tokenization and word-grained tokenization method. The metric is top-1 accuracy (%) of zero-shot image classification. The better result is highlighted with **bold**.

| Model \ Dataset | CIFAR10 | CIFAR100 | Caltech101 | Caltech256 | DTD | Sports | Flowers | SUN397 | EuroSAT | ImageNet | Average |
|-------------------------|------------------------------|-------------|-------------|-------------|-------------|-------------|-------------|-------------|---------|-------------|--------------|
| | Wukong _{ViT-B-Word} | 89.1 | 62.1 | 88.7 | 80.8 | 29.1 | 93.7 | 53.3 | 49.6 | 36.2 | 43.9 |
| Wukong _{ViT-B} | 87.1 | 62.6 | 89.1 | 82.3 | 37.3 | 95.6 | 64.8 | 56.0 | 32.6 | 49.1 | 65.65 |

fine-grained textual tokens. A typical example from the Chinese ImageNet dataset is that the word “蜂鸟”(hummingbird) consists of two characters: “蜂”(bee) and “鸟”(bird).

C.2 Visualization of Word-patch Alignment

Since we follow the fine-grained interaction in FILIP [53], our trained models FILIP_{ViT-L} and FILIP_{Swin-L} likewise own the capability of capturing the correspondence between images and texts. Note that they are trained using the token-wise similarity. We exclude ones with the global similarity since they lack of word-patch alignment capability, which has been evidenced in previous work [53].

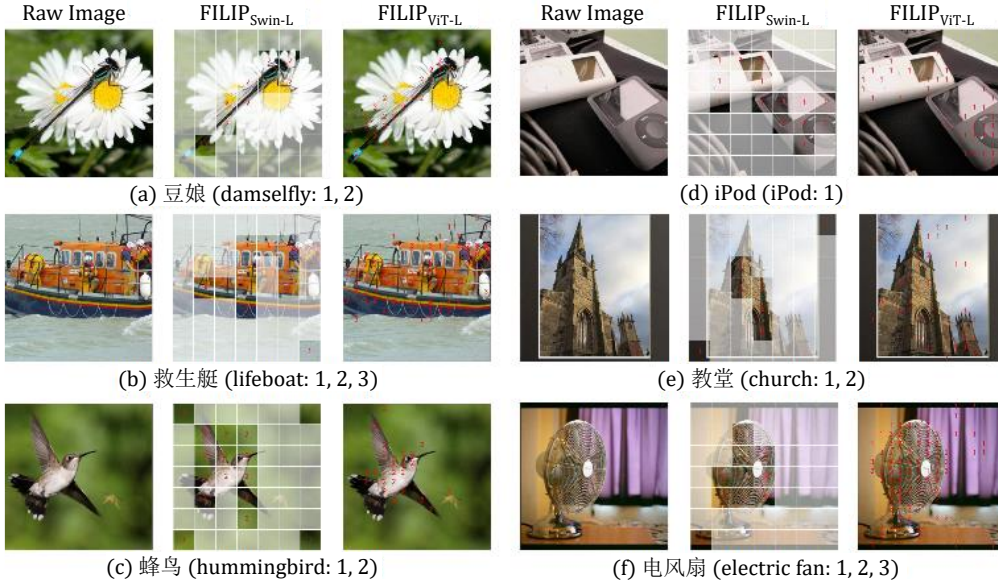


Figure 6: Visualization of word-patch alignment. We randomly choose six classes in the Chinese ImageNet dataset. Each Chinese label name is used as a prompt, whose English text is described in the parentheses. Behind which, the tail numbers indicate the location indices of this class label in the tokenized textual input. Take (a) as an example, the number 0 always represents [CLS], the number 1 is the tokenized “豆” and the number 2 is “娘”. Indices of the tokenized label name are highlighted in red.

As shown in Figure 6, we visualize images from six labels in the Chinese ImageNet. We apply the same visualization method as FILIP [53], to align textual tokens and image patch tokens. In particular, we calculate the token-wise similarity between each image patch token and all tokenized textual tokens from the text label, i.e., [CLS] {class label tokens} [SEP]. For each image patch, the position index of textual tokens with the maximum similarity is considered as its predicted text token. Note that the Chinese class label is often tokenized to more than one token. We highlight all the predicted position indices that correspond to the class label, and place them at the center of the corresponding patches.

From Figure 6, we surprisingly find that both models are able to predict image patches of the target object. For $FILIP_{ViT-L}$ with each image patchified to 16×16 , such word-patch alignment is more fine-grained than $FILIP_{Swin-L}$ with the output resolution as 7×7 . Take Figure 6 (e) as an example, $FILIP_{ViT-L}$ is even able to align Chinese tokens “教” and “堂”, which means church as one word, to the smaller church in the bottom-right corner. $FILIP_{ViT-L}$ also well outlines the hummingbird in the example of Figure 6 (c), while $FILIP_{Swin-L}$ often aligns to the main body of the target object. Another interesting observation is that these Chinese pre-trained models are able to align image patches to English tokens as shown in Figure 6 (d). The main reason lies in that the vocabulary used from BERT [7] also includes multilingual words such as “iPod”.

Overall, this visualization confirms that our released models pre-trained on Wukong dataset indeed learn the correspondence between images and Chinese texts, or even in a more finer-grained manner, the alignment between image patches and words. This capability of aligning words and patches offers a potential solution for image object localization.

D Downstream Datasets

D.1 Prompt Template

As previously observed in GPT-3 [1], the zero-shot performance can be significantly improved by customizing the prompt templates to each task. CLIP [35] also shows that specifying the category for each dataset contributes to the performance. However, since we only aim to provide a Chinese dataset with a general benchmarking of our released models, we leave the “prompt engineering” to the future work. We simply use the reported 80 general English prompts in CLIP and translate them to Chinese manually, as follows. Note that “{}” is replaced by the exact Chinese label name. We release these Chinese prompts for future fair comparison in the community. Below are all the 80 Chinese prompts and the corresponding English prompts.

Chinese Prompts: “{}的照片。”，“许多{}的照片。”，“一张包含{}的照片。”，“质量差的{}的照片。”，“{}的雕塑。”，“难以看到{}的照片。”，“{}的低分辨率照片。”，“{}的渲染。”，“涂鸦{}。”，“{}的糟糕照片。”，“{}的裁剪照片。”，“{}的纹身。”，“{}的刺绣照片。”，“很难看到{}的照片。”，“{}的明亮照片。”，“一张干净的{}的照片。”，“{}的深色照片。”，“{}的手绘画。”，“我的{}的照片。”，“不自然的{}的照片。”，“一张酷的{}的照片。”，“{}的特写照片。”，“{}的黑白照片。”，“一幅{}的画。”，“一幅{}的绘画。”，“一张{}的像素照片。”，“{}的雕像。”，“一张{}的明亮照片。”，“{}的裁剪照片。”，“人造的{}的照片。”，“一张关于{}的照片。”，“损坏的{}的jpeg照片。”，“{}的模糊照片。”，“{}的相片。”，“一张{}的好照片。”，“{}的渲染照。”，“视频游戏中的{}。”，“一张{}的照片。”，“{}的涂鸦。”，“{}的近距离照片。”，“{}的折纸。”，“{}在视频游戏中。”，“{}的草图。”，“{}的涂鸦照。”，“{}的折纸形状。”，“低分辨率的{}的照片。”，“玩具{}。”，“{}的副本。”，“{}的干净的照片。”，“一张大{}的照片。”，“{}的重现。”，“一张漂亮的{}的照片。”，“一张奇怪的{}的照片。”，“模糊的{}的照片。”，“卡通{}。”，“{}的艺术作品。”，“{}的素描。”，“刺绣{}。”，“{}的像素照。”，“{}的拍照。”，“{}的损坏的照片。”，“高质量的{}的照片。”，“毛绒玩具{}。”，“漂亮的{}的照片。”，“小{}的照片。”，“照片是奇怪的{}。”，“漫画{}。”，“{}的艺术照。”，“{}的图形。”，“大{}的照片。”，“黑白的{}的照片。”，“{}毛绒玩具。”，“一张{}的深色照片。”，“{}的摄影图。”，“{}的涂鸦照。”，“玩具形状的{}。”，“拍了{}的照片。”，“酷酷的{}的照片。”，“照片里的小{}。”，“{}的刺青。”

English Prompts: “a photo of a {}.”，“a bad photo of a {}.”，“a photo of many {}.”，“a sculpture of a {}.”，“a photo of the hard to see {}.”，“a low resolution photo of the {}.”，“a rendering of a {}.”，“graffiti of a {}.”，“a bad photo of the {}.”，“a cropped photo of the {}.”，“a tattoo of a {}.”，“the embroidered {}.”，“a photo of a hard to see {}.”，“a bright photo of a {}.”，“a photo of a clean {}.”，“a photo of a dirty {}.”，“a dark photo of the {}.”，“a drawing of a {}.”，“a photo of my {}.”，“the plastic {}.”，“a photo of the cool {}.”，“a close-up photo of a {}.”，“a black and white photo of the {}.”，“a painting of the {}.”，“a painting of a {}.”，“a pixelated photo of the {}.”，“a sculpture of the {}.”，“a bright photo of the {}.”，“a cropped photo of a {}.”，“a plastic {}.”，“a photo of the dirty {}.”，“a jpeg corrupted photo of a {}.”，“a blurry photo of the {}.”，“a photo of the {}.”，“a good photo of the {}.”，“a rendering of the {}.”，“a {} in a video game.”，“a photo of one {}.”，“a doodle of a {}.”，“a close-up photo of the {}.”，“the origami {}.”，“the {} in a video game.”，“a sketch of a {}.”，“a doodle of the {}.”，“a origami {}.”，“a low resolution photo of a {}.”，“the toy {}.”，“a rendition of the {}.”，“a photo of the clean {}.”，“a photo of a large {}.”，“a rendition of a {}.”，“a photo of a nice {}.”，“a

photo of a weird {}.", "a blurry photo of a {}.", "a cartoon {}.", "art of a {}.", "a sketch of the {}.", "a embroidered {}.", "a pixelated photo of a {}.", "itap of the {}.", "a jpeg corrupted photo of the {}.", "a good photo of a {}.", "a plushie {}.", "a photo of the nice {}.", "a photo of the small {}.", "a photo of the weird {}.", "the cartoon {}.", "art of the {}.", "a drawing of the {}.", "a photo of the large {}.", "a black and white photo of a {}.", "the plushie {}.", "a dark photo of a {}.", "itap of a {}.", "graffiti of the {}.", "a toy {}.", "itap of my {}.", "a photo of a cool {}.", "a photo of a small {}.", "a tattoo of the {}."

D.2 Datasets for Image-text Retrieval

The data scale of datasets for image-text retrieval is described in Table 10. The texts in Flickr8K-CN, COCO-CN, AIC-ICC are human-annotated, the texts in Flickr30K-CN train/val set are machine-translated while the texts in Flickr30K-CN test set are human-translated from their original English counterparts. In Flickr8K-CN, Flickr30K-CN and AIC-ICC, each image is paired with 5 texts. In COCO-CN, each image is paired with 1 to 2 texts. In MUGE, each text is paired with 1 to 2 images in the train set, and with about 6 images in the val/test sets.

Table 10: Statistics of each image-text retrieval dataset.

| Dataset | split | #Images | #Sentences |
|-------------------|--------|---------|------------|
| Flickr8K-CN [20] | train | 6,000 | 30,000 |
| | val | 1,000 | 5,000 |
| | test | 1,000 | 5,000 |
| Flickr30K-CN [18] | train | 29,783 | 148,915 |
| | val | 1,000 | 5,000 |
| | test | 1,000 | 5,000 |
| COCO-CN [21] | train | 18,341 | 20,065 |
| | val | 1,000 | 1,100 |
| | test | 1,000 | 1,053 |
| AIC-ICC [51] | train | 210,000 | 1,050,000 |
| | val | 30,000 | 150,000 |
| | test-1 | 30,000 | 150,000 |
| | test-2 | 30,000 | 150,000 |
| MUGE [22] | train | 129,380 | 248,786 |
| | val | 29,806 | 5,008 |
| | test | 30,399 | 5,004 |
| Wukong-Test | val | 33,365 | 33,365 |

E Limitations and Societal Impacts

Wukong dataset might only contain the current concepts and language expression at the time of collection. Since language evolves with human activities, our dataset certainly cannot cover the newly emerging concepts, words and language expression in the future. It is the same case for the image data side, where the new visual object or design can not be covered. However, fine-tuning pre-trained models on these up-to-date data is able to address this issue. In addition, our dataset is built on the corpora from Chinese Internet, which means the vocabulary and expression may more or less fit into the Chinese culture. Also, there is more written language than spoken language and it might bring bias at some point. Another limitation is the absence of very long texts in our dataset. Therefore, the ability of understanding documents using our released models might be limited. Furthermore, in terms of societal impacts, our dataset is built in a general purpose with images and texts collected from unlimited domains. Models trained on this dataset might express some undesirable and uncontrollable tendencies in terms of image-text correspondence. Therefore, although our released models are discriminative, special attention is still suggested in practical use.

F Hosting and Maintenance Plan

Long-term maintenance of Wukong, as well as Wukong-Test, and models proposed and evaluated in our paper will be made by the authors. The dataset website containing introductions, benchmarks, terms of use and any possible improvement in the future are hosted in Github Pages which is a widely-used website hosting service. In terms of content hosting, there are three parts: code, models and datasets. All of them are hosted on open platforms that each individual is able to download freely. For evaluation code, Pytorch version is hosted on Github and Mindspore version is hosted on Gitee, an open-source code hosting platform specialized for Chinese users. The model checkpoints trained in our paper are hosted on Google Drive. The datasets including Wukong and Wukong-Test are hosted on Google Drive and Baidu Cloud, a widely-used cloud storage service in China, as backup.

G License

Unless specifically labeled otherwise, our released datasets are provided to You under the terms of the Creative Commons Attribution-NonCommercial-ShareAlike 4.0 International Public License (“CC BY-NC-SA 4.0”), with the additional terms included herein. The CC BY-NC-SA 4.0 may be accessed at <https://creativecommons.org/licenses/by-nc-sa/4.0/legalcode>. When You download or use the datasets from our website or elsewhere, You are agreeing to comply with the terms of CC BY-NC-SA 4.0, and also agreeing to the dataset Terms. Where these dataset Terms conflict with the terms of CC BY-NC-SA 4.0, these dataset Terms shall prevail. We reiterate once again that this dataset is used only for non-commercial purposes such as academic research, teaching, or scientific publications. We prohibits You from using the dataset or any derivative works for commercial purposes, such as selling data or using it for commercial gain.